Interface Components: Nanoparticles, Colloids, Emulsions, Surfactants, Proteins, Polymers

Measuring the Adhesion Forces for the Multivalent Binding of Vancomycin-conjugated Dendrimer to Bacterial Cell-Wall Peptide

Elizabeth Peterson, Christine Joseph, Hannah Peterson, Rachael Bouwman, Shengzhuang Tang, Jayme Cannon, Kumar Sinniah, and Seok Ki Choi

Langmuir, **Just Accepted Manuscript** • DOI: 10.1021/acs.langmuir.8b01137 • Publication Date (Web): 24 May 2018

Measuring the Adhesion Forces for the Multivalent Binding of Vancomycin-conjugated Dendrimer to Bacterial Cell-Wall Peptide

Elizabeth Peterson,[§] Christine Joseph,[†] Hannah Peterson,[§] Rachael Bouwman,[§] Shengzhuang Tang,[†,‡] Jayme Cannon,[†,‡] Kumar Sinniah,[§] and Seok Ki Choi*[†,‡]*

[†]Michigan Nanotechnology Institute for Medicine and Biological Sciences, and [‡]Department of Internal Medicine, University of Michigan Medical School, Ann Arbor, MI 48109, United States

[§]Department of Chemistry & Biochemistry, Calvin College, Grand Rapids, MI 49546, United States

*To whom correspondence should be addressed,

Phone: (616) 526-6058; Fax: (616) 526-6501; Email: ksinniah@calvin.edu

Phone: (734) 647-0052; Fax: (734) 936-2990; Email: skchoi@umich.edu

ABSTRACT

Multivalent ligand-receptor interaction provides the fundamental basis for the hypothetical notion that high binding avidity relates to the strong force of adhesion. Despite its increasing importance in the design of targeted nanoconjugates, an understanding of the physical forces underlying the multivalent interaction remains a subject of urgent investigation. In this study, we designed three vancomycin (Van)-conjugated dendrimers G5(Van)$_n$ (n = mean valency = 0, 1, 4) for bacterial targeting with generation 5 (G5) poly(amidoamine) dendrimer as a multivalent scaffold, and evaluated both their binding avidity and physical force of adhesion to a bacterial model surface by employing surface plasmon resonance (SPR) spectroscopy and atomic force microscopy (AFM). The SPR experiment for these conjugates was performed in a biosensor chip surface immobilized with a bacterial cell-wall peptide Lys-D-Ala-D-Ala. Of these, G5(Van)$_4$ bound most tightly with K_D of 0.34 nM, which represents an increase in avidity by two or three orders of magnitude relative to a monovalent conjugate G5(Van)$_1$ or free vancomycin, respectively. By single molecule force spectroscopy, we measured the adhesion force between G5(Van)$_n$ and the same cell-wall peptide immobilized on the surface. The distribution of adhesion forces increased in proportion to vancomycin valency with the mean force of 134 pN at n = 4 greater than 96 pN at n = 1 at a loading rate of 5200 pN/s. In summary, our results are strongly supportive of the positive correlation between the avidity and adhesion force in the multivalent interaction of vancomycin nanoconjugates.

Key Words: Vancomycin, Multivalent Avidity, Adhesion Force, Surface Plasmon Resonance Spectroscopy, Atomic Force Spectroscopy

Introduction

The multivalent ligand strategy constitutes one of the fundamental concepts underlying the function of multifunctional nanoparticles (NPs) designed for therapeutic, diagnostic and biomedical applications.[1-4] In this design, each multivalent NP is attached with multiple copies of a ligand in order to bind tightly and selectively to its target cell. This multivalent effect, which correlates high binding avidity with ligand multivalency, is supported by numerous biochemical and biophysical studies of protein-ligand interaction and NP-cell adhesion.[5-11] Furthermore, it offers targeting specificity which has played a key role in the design of many classes of multifunctional NPs based on highly branched dendrimer polymers,[12-14] polymer micelles,[15] and functional inorganic NPs such as gold NPs (AuNPs),[16-18] iron oxide NPs (IONPs),[19, 20] and upconversion nanocrystals (UCNs).[21-23]

In addition, the multivalent binding is hypothesized to confer the strong force of adhesion[24-28] by which each NP remains firmly bound to the surface of its target under a shear flow. Ability for such adhesion is considered to be highly critical in *in vivo* applications as they occur under a continuous flow condition.[29] Despite such significance, physical forces that relate to multivalent binding avidity remain largely undefined in most multivalent NPs. Currently, only a few studies reported the forces of multivalent adhesion, such as those associated with uropathogenic *E. coli*[28] and tumor biomarkers.[24-26] Here, we are interested in measuring adhesion forces which relate to the multivalent binding of a vancomycin-conjugated dendrimer to a bacterial model surface.

This multivalent strategy has been applied in the development of bacteria-targeting NPs.[19, 30-32] Each bacterial cell presents a number of cell wall components in its outer surface which are targetable by small molecule ligands which include a bis(di-picolylamine)-zinc complex[30, 33] and

by cell wall-specific drug molecules such as polymyxin,[34-37] and vancomycin.[38-40] Of these, vancomycin offers a unique ability for targeting Gram(+) bacterial pathogens due to its specific affinity (dissociation constant, $K_D \approx 10^{-6}$ M)[19, 39, 41] to a D-Ala-D-Ala precursor in the cell wall (Figure 1).[42, 43] Thus, vancomycin-conjugated NPs were designed for bacterial targeting by the covalent attachment of multiple vancomycin molecules on the surface of inorganic NPs[31, 32, 44] or on the scaffold of polymer molecules.[19, 38, 45] Each of these NPs was noted for displaying an ability for high targeting efficiency,[19, 38] bacterial capture,[19, 32] and potent antibacterial activity.[44, 45]

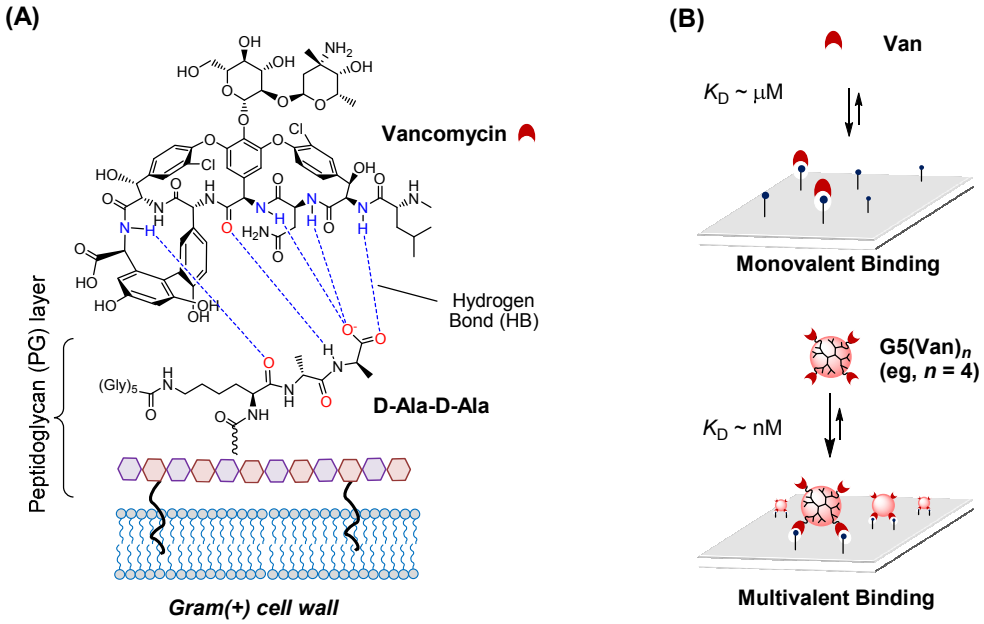

Figure 1. (A) Mechanism for the binding of a bacterial cell-wall peptide precursor, D-Ala-D-Ala, by vancomycin through a network of five hydrogen bond (HB) interactions. (B) A schematic illustrating a much tighter binding ($K_D \geq 10^{-9}$ M) by a multivalent vancomycin conjugate than vancomycin ($K_D \approx 10^{-6}$ M) on the surface. The conjugate, G5(Van)$_n$ refers to a fifth generation (G5) PAMAM dendrimer conjugated with a mean valency (n) of vancomycin.

In our prior study,[19] we used a fifth generation (G5) poly(amidoamine) (PAMAM) dendrimer (diameter 5.4 nm)[46] as a multivalent scaffold for vancomycin conjugation. As a highly branched, monodisperse polymer molecule, this dendrimer G5$(NH_2)_n$ has a large number of peripheral branches (theoretical n = 128),[46] each amine-terminated and chemically amenable for ligand or drug conjugation for targeted applications in cancers and inflammatory diseases[47-50] as illustrated by G5 dendrimers conjugated with folic acid,[13, 14, 17, 49, 51] riboflavin,[52] lactobionic acid,[12] and RGD.[16, 53] This study designed a series of multivalent vancomycin conjugates G5$(Van)_n$ (n = 1–6; Van = vancomycin),[19] and investigated their binding avidity (K_D) to a model surface presenting Lys-D-Ala-D-Ala by surface plasmon resonance (SPR) spectroscopy. It demonstrated the dependence of binding avidity on vancomycin valency (n) with a threshold valency (n) of 2 required for low nM binding avidity.

This current study aims to investigate whether multivalent avidity relates to strong adhesion forces in the binding of G5$(Van)_n$ (n = 0, 1, 4) to a surface immobilized with a cell-wall peptide molecule. Two comparative biophysical methods are employed in this study: SPR spectroscopy and atomic force microscopy (AFM). First, SPR is selected because it allows the investigation of receptor-ligand interaction under a flow condition.[54] Thus, it enables us to quantitatively determine K_D values for the multivalent interaction between the dendrimer conjugate and the peptide in the surface.[19, 35, 38, 41] Second, AFM constitutes one of the standard methods which is applicable for measuring the physical forces of biological relevance.[28, 55] Its application has played a critical role in advancing our understanding of physical forces involved in biomolecular interactions.[27, 56-58] In a previous AFM study, we measured rupture forces associated with a multivalent cooperative interaction between a riboflavin-conjugated multivalent dendrimer and a riboflavin receptor immobilized on the surface.[25] Here, this current study is focused on adhesion

forces associated with the interaction by vancomycin-conjugated dendrimers. In summary, this study presents evidence that relates strong adhesion forces to high avidity binding by cell-wall targeting multivalent conjugates.

RESULTS AND DISCUSSION

Synthesis and Characterization of Dendrimer Conjugates. As summarized in Scheme 1, we designed multivalent dendrimers by the amide conjugation of G5 dendrimer G5$(NH_2)_n$ (n = 114 determined by potentiometric titration[59]) with vancomycin at its C-terminus with the variation of multivalency.[19] In this design strategy, the dendrimer was also co-conjugated with (±)-α-lipoic acid for use later as an anchoring moiety to an AFM tip coated with gold (Au) by which its cyclic disulfide handle allows the dendrimer conjugate to be chemisorbed to the tip surface through Au-S bond formation.[60]

First, we prepared **1** G5$(LA)_m$ (LA – α-Lipoic amide) by reacting G5$(NH_2)_{114}$ with an activated *N*-hydroxybenzotriazole (HOBt) ester of lipoic acid (LA) added at a ratio of 15 molar equivalent to the dendrimer. Subsequently after this treatment, unreacted peripheral amines which remained in G5$(LA)_m$ were allowed to react with vancomycin, which was added as its pre-activated HOBt ester form. The ratio of the pre-activated vancomycin to the dendrimer ([Van]/[G5]) varied from 0, 2, or 8 in order to vary the vancomycin valency of the resulting conjugate. Finally, each of the unreacted amines left on the dendrimer reacted exhaustively with glutaric anhydride for conversion to an *N*-glutaryl amide, rendering the dendrimer particle fully covered with glutarate moieties in the peripheral surface. Such surface modification is beneficial as each glutarate group (pK_a 4.5) is negatively charged under physiological condition, and it helps prevent an undesired attractive electrostatic interaction occurring between the conjugate

surface and an individual cell-wall peptide which is terminated with a negatively-charged carboxylate.

Scheme 1. Synthesis of vancomycin (Van)-conjugated G5 PAMAM dendrimers **2**–**4** G5(LA)$_{m=11}$(Van)$_n$ (top), and Poisson distribution of dendrimer populations for **3** and **4** with regards to the valency of vancomycin (bottom). Note that only a fraction of the terminal branches per dendrimer (theoretical 128)[46] are shown for clarity.

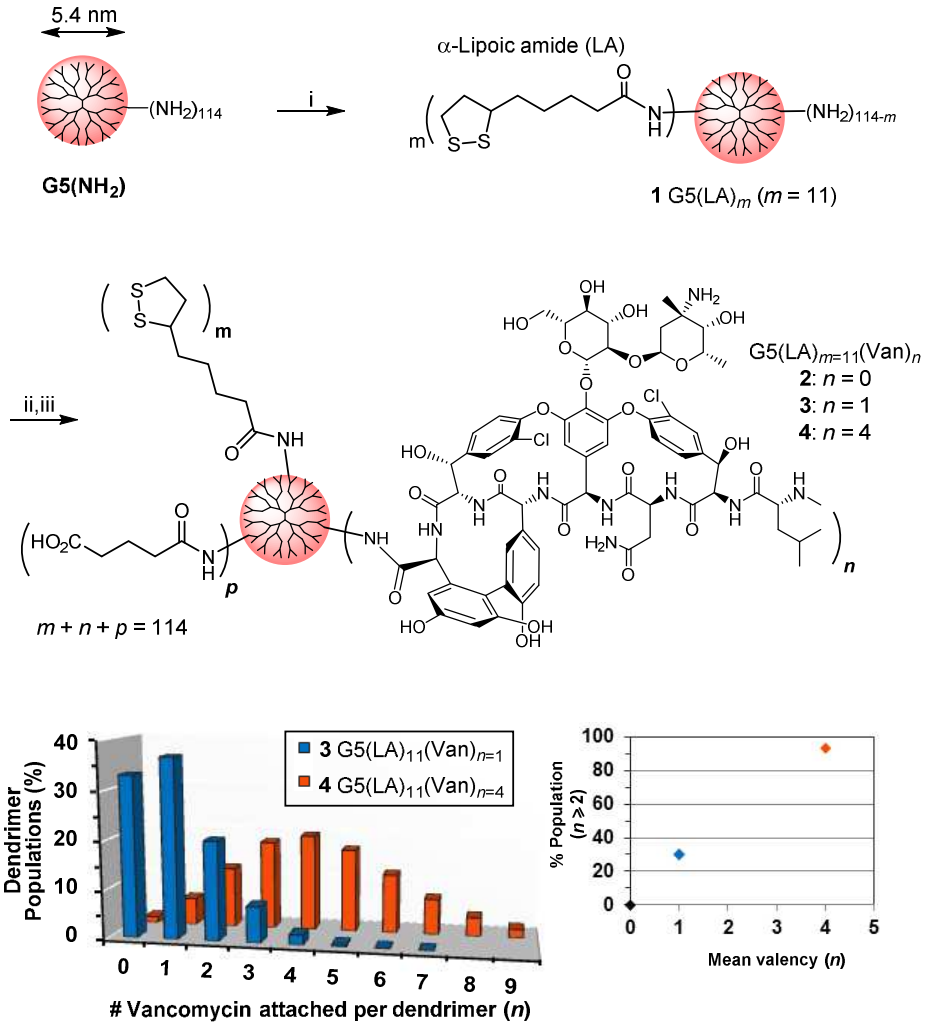

Reagents and conditions: (i) (±)-α-Lipoic acid (15 equiv), EDC, HOBt, DIPEA, room temp; (ii) vancomycin hydrochloride, DIPEA, HOBt, PyBOP, DMSO, DMF, 30 min, room temp; then added to dendrimer ([vancomycin]/[G5] = 0, 2, or 8), MeOH, 12 h; (iii) Glutaric anhydride (150

equiv), DIPEA (200 equiv), 12 h, room temp. Abbreviations: EDC = *N*-(3-dimethylaminopropyl)-*N*′-ethylcarbodiimide hydrochloride, HOBt = 1-hydroxybenzotriazole, DIPEA = *N*,*N*′-diisopropyl-*N*-ethylamine, PyBOP = benzotriazol-1-yl-oxytripyrrolidinophosphonium hexafluorophosphate, LA = α-Lipoic amide

Each of the conjugates **2**–**4** G5(LA)$_m$(Van)$_n$ was purified by dialysis in a membrane tubing (molecular weight cut-off or MWCO 10,000 Da). Its homogeneity was determined by UPLC analysis, which indicated ≥95% of purity on a polymer basis (Figure S1). In addition, each conjugate was confirmed for its homogeneity using gel permeation chromatography (GPC) as shown in Figure S1. Each of these conjugates was fully characterized for their identity by various analytical methods. These conjugates were fully characterized for their identity, hydrodynamic diameter (D_h), and surface charges (ZP) by various analytical methods as summarized in Table 1. ^{1}H NMR spectral data of these conjugates showed characteristic signals specifically assigned to the protons of LA and vancomycin (Figure S2, S3). UV–vis absorption spectroscopy of **3** and **4** (Figure S1) showed a strong absorption at 282 nm by vancomycin with a value of molar absorptivity (ε = 6,652 $M^{-1} \times cm^{-1}$) which is in a close agreement with a reported value.[19] The relative molar mass (M_r) of each conjugate was measured by matrix assisted laser desorption ionization time-of-flight (MALDI–ToF) spectrometry as summarized in Table 1, and it was used to calculate the mean valency of vancomycin attached.

Table 1. Macromolecular properties of dendrimer conjugates 2–4 G5(LA)$_m$(Van)$_n$

Conjugate	M_r (g × mol^{-1})[a]	m[b]	n[c]	ZP (mV)[d]	D_h (nm)[e]
G5(NH$_2$)$_{114}$	27,600	-	-	35.5(±9.5)	5.3(±0.2)
2	36,600	11(±1)	-	−55.4(±3.4)	14.6(±3.8)
3	36,900	11(±1)	1(±0.02)	−57.5(±4.6)	16.7(±0.1)

4	41,600	11(±1)	4(±0.01)	−56.5(±4.8)	9.5(±1.2)

[a] Measured by matrix assisted laser desorption ionization (MALDI)–time of flight (ToF) mass spectrometry

[b] Mean value determined by ^{1}H NMR spectroscopy

[c] Mean value determined by UV–vis spectrometry

[d] Zeta potential (ZP) measured in 1.0 mM HEPES, pH 7.0 ([dendrimer] = 1.0 mg/mL)

[e] Number-weighted hydrodynamic diameter measured by dynamic light scattering (DLS) in phosphate buffered saline (PBS), pH 7.4 ([dendrimer] = 0.1 mg/mL)

Ligand Valency and Distribution. The valency (*m*) of the lipoic amide molecule attached to the conjugate G5(LA)$_m$(Van)$_n$ was determined as m = 11 (±1) on a mean basis by an NMR integration method.[60] Here the area under curve (AUC) of CH_2 signals for LA (δ 1.0–1.4 ppm) was compared to the AUC of reference CH_2 signals from glutaryl amide (GA; δ 1.7, 2.0–2.2 ppm): m + p = 114, and m/p = AUC_{LA}/AUC_{GA} where m and p refer to the mean number of LA and GA residues, respectively. The valency (*n*) of vancomycin molecules attached to each conjugate is reported on a mean basis which was calculated by the analysis of UV–vis absorptivity at 282 nm (vancomycin) as described in our prior work:[19] n = 1 (**3**); n = 4 (**4**). The efficiency for vancomycin conjugation ($[Van]_{attached} \div [Van]_{added}$) is 0.5 for each conjugate; this might be attributable, in part, to the incomplete activation of vancomycin *in situ* and/or the potential impact by pre-attached LA residues through steric hindrance on the approach of a relatively bulky vancomycin molecule to the dendrimer surface.

An amide coupling reaction used for ligand conjugation occurs in a stochastic manner on the surface of a nanoparticle,[61] which leads to a distribution of conjugate populations which present a variable range of ligand valency. We calculated the distribution of dendrimer populations with regards to vancomycin valency for **2** and **3** G5(LA)$_{m=11}$(Van)$_n$ (n = 1, 4) according to Poissonian

simulation.[61] The plot in Scheme 1 (bottom) shows that, despite its average valency of 1, conjugate **2** is not entirely composed of a monovalent species (n = 1; 37%). Instead, its distribution includes the non-conjugated dendrimer (n = 0; 33%) and a divalent conjugate species (n = 2; 20%). However, the other conjugate **3** represents mostly multivalent species (n = 2–9; 93%; median = 4.5). Despite their valency distribution, the three conjugates **2** – **4** remain similar in the surface charge (ZP = −55.4 to −57.5) as summarized in Table 1. However, they show a large difference in the hydrodynamic size (D_h) such that the higher-valent conjugate **4** (9.5 nm) is smaller than **2** (14.6 nm) or **3** (16.7 nm). This might be attributable to the hydrophobic collapse of the bulky vancomycin molecule to the peripheral space of the dendrimer through the embedding or encapsulation[14, 16, 50, 53] of its lipophilic residues.

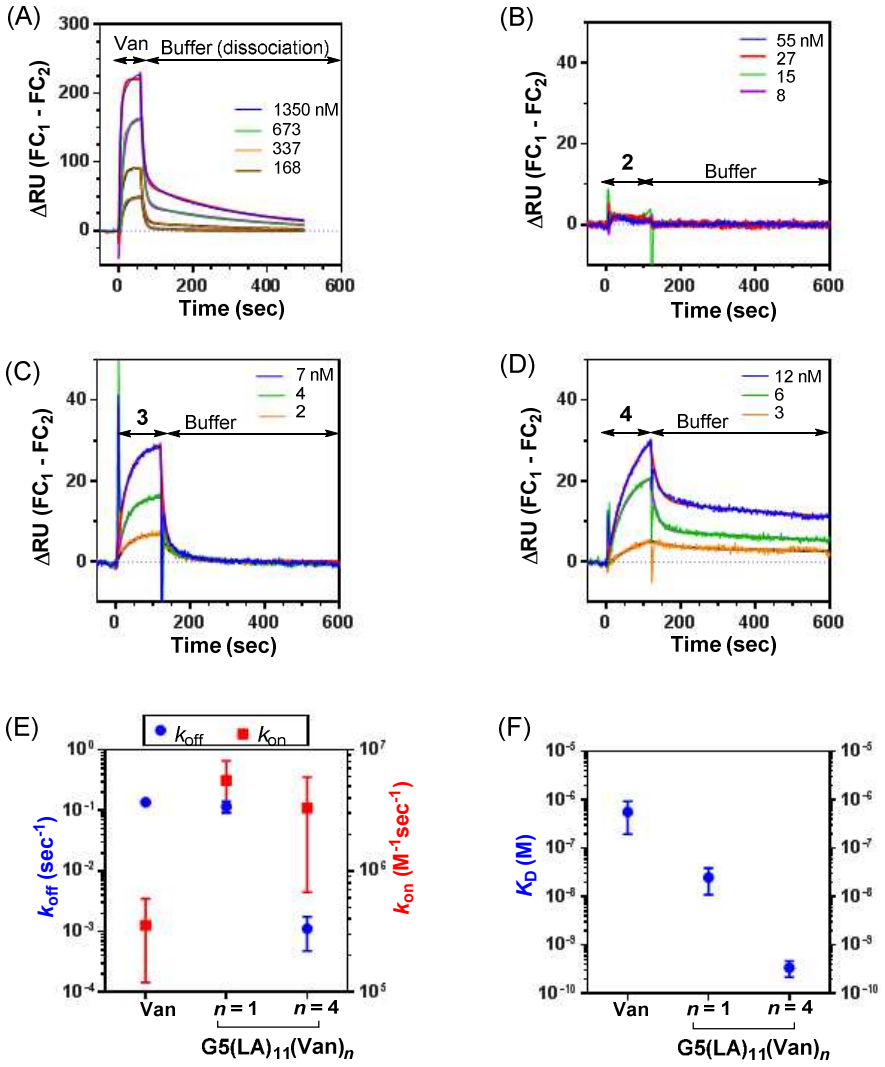

Figure 2. (A–D) Surface plasmon resonance (SPR) sensorgrams for the binding kinetics of **2**–**4** G5(LA)$_{11}$(Van)$_n$ (n = 0, 1, 4) to a bacterial model surface prepared by immobilization of N^{α}-Ac-Lys-D-Ala-D-Ala on the CM5 sensor chip. Simulated curves are shown as overlaid in each plot. (E) Rate constants for dissociation (k_{off}) and association (k_{on}) extracted from the SPR data (above). (F) Values of K_D (= k_{off}/k_{on}) calculated for G5(LA)$_{11}$(Van)$_n$ plotted as a function of mean valency (n). Values for free vancomycin are provided as the reference indicative for its monovalent association. Mean ± SD (N ≥ 3).

SPR Spectroscopy. We performed SPR spectroscopy to determine the K_D values of conjugates **2**–**4** to the D-Ala-D-Ala ligand presented in a model surface for Gram(+) cell walls. This surface was prepared by the immobilization of N^{α}-Ac-Lys-D-Ala-D-Ala in a CM5 sensor chip following an amide coupling method[19, 35] which led to the immobilization of the cell wall peptide at a surface density of 1.6×10^{-13} mole/mm^2 (equivalent to 9.9×10^{10} molecules/mm^2).

Vancomycin was investigated for its dose-dependent binding kinetics (Figure 2A). Its rate constants for dissociation (k_{off}) and association (k_{on}) were extracted by the Langmuir analysis of each sensorgram,[54] and were used to calculate its equilibrium dissociation constant K_D (= k_{off}/k_{on}). Its K_D value of 5.7×10^{-7} M (Table 2) is in good agreement with prior values determined by SPR and other biophysical methods ($K_D = 10^{-7} – 10^{-6}$ M).[19, 39, 41]

Monovalent Affinity vs. Multivalent Avidity. Each of three conjugates G5(LA)$_{11}$(Van)$_n$ **2** (n = 0), **3** (n = 1) and **4** (n = 4) which differ only in vancomycin valency was investigated for its binding kinetics using the same sensor chip. G5(LA)$_{11}$ **2** showed lack of binding to the peptide surface as anticipated as a control dendrimer which has no vancomycin conjugated (Figure 2B). This result suggests the lack of nonspecific binding by the conjugate as well. G5(LA)$_{11}$(Van)$_{n=1}$ **3** was studied for its binding in the range of low nM concentrations ([**3**] = 2–7 nM), and its SPR sensorgrams acquired illustrate its concentration-dependent binding (Figure 2C). Compared to vancomycin, its dissociation rate remains almost identical (k_{off}), while its association (k_{on}) occurs approximately 10-fold faster than vancomycin (Figure 2E). As a result, **3** showed a K_D value of 2.5×10^{-8} M which represents a 23-fold enhancement in its affinity (Figure 2F, Table 2). Such faster association (k_{on}) by **3** is attributable to the combination of two kinetic events which could occur cooperatively: (i) the primary vancomycin-peptide interaction to form a complex on the

surface; (ii) the secondary dendrimer-surface interaction that enables to convert the complex to form more stable complexes (the surface conversion mechanism).[62]

Table 2. Kinetic rate constants and dissociation constant K_D determined for the binding of **2**–**4** $G5(LA)_{11}(Van)_n$ to the D-Ala-D-Ala surface by SPR spectroscopy.

Conjugate	Valency (n)	k_{off} (s^{-1})[a]	k_{on} ($M^{-1} \times s^{-1}$)[a]	K_D (M)[b]	β[c]
Vancomycin	1	$1.4(\pm0.1) \times 10^{-1}$	$3.6(\pm2.4) \times 10^{5}$	5.7×10^{-7}	1
2	0	-	-	-	-
3	1	$1.2(\pm0.2) \times 10^{-1}$	$5.6(\pm2.5) \times 10^{6}$	2.5×10^{-8}	23 (23[d])
4	4	$1.1(\pm0.6) \times 10^{-3}$	$3.3(\pm2.7) \times 10^{6}$	3.4×10^{-10}	1676 (419[d])

[a] The value within parentheses refers to standard deviation.

[b] Each value represents an average of K_D ($= k_{off}/k_{on}$) calculated from multiple injection concentrations ($N \geq 4$).

[c] β = multivalent binding enhancement = K_D(Van) ÷ K_D(Conjugate)

[d] Corrected for the valency (β ÷ n)

$G5(LA)_{11}(Van)_{n\,=\,4}$ **4** was also studied for binding at the similar range of concentrations (Figure 2D). It showed a distinct feature in its dissociation phase which is characterized by a much slower dissociation than vancomycin or **3**. A kinetic analysis performed for each sensorgram suggested two populations of bound dendrimer species. A majority (≥60%) of its bound populations displayed a k_{off} of 1.1×10^{-3} s^{-1}, which is indicative of 100-fold slower dissociation than vancomycin or **3.** A minor fraction (≤40%) showed a slightly faster dissociation with k_{off} of 5.4×10^{-2} s^{-1} (not shown). Such slower dissociation is reported frequently in multivalent ligand-receptor systems and is considered the hallmark of tight multivalent binding.[5-

[7] Its slower dissociation contributed to higher avidity for **4** (K_D = 0.34 nM) than vancomycin or **3** with a multivalent binding enhancement (β) factor of 1676 or 74 relative to vancomycin or **3**, respectively (Table 2).

In summary, the multivalent conjugate **4** shows an enhancement in avidity by two to three orders of magnitude to vancomycin or a monovalent conjugate, which is fully consistent with our prior work.[19] While its high β value is not directly indicative of its multivalent cooperativity factor (α),[7] its high avidity could serve as a basis for its tight adhesion force to the ligand-immobilized surface. In the next section, we employed atomic force microscopy to determine the physical force involved in its multivalent binding.

AFM spectroscopy. The force between a dendrimer conjugate and the D-Ala-D-Ala surface was measured using an AFM probe and a flat gold substrate which presented **5** α-LA-Lys-D-Ala-D-Ala on its surface. For this purpose, each AFM probe was prepared for each conjugate **2**–**4** by the surface modification of a gold-coated AFM tip with the conjugate through Au-thiol chemisorption.[25] As the method is well established for the immobilization of a disulfide-containing small molecule or a biomacromolecule on the gold surface,[58, 63-66] the chemisorption occurred between the cyclic disulfide terminus of an α-lipoic amide moiety attached to the conjugate and the tip surface as shown in Scheme 2. The peptide-immobilized gold substrate was prepared similarly but independently from the gold tip through the Au-thiol chemisorption of **5** α-LA-Lys-D-Ala-D-Ala to the surface of a flat gold substrate.

Scheme 2. Preparation of an AFM probe tip (A) and a substrate presenting a layer of α-LA-Lys-D-Ala-D-Ala as the cell-wall peptide (B). In each preparation, the attachment of the dendrimer or the peptide to the surface occurs covalently via Au-thiol chemisorption from α-lipoic amide (LA).

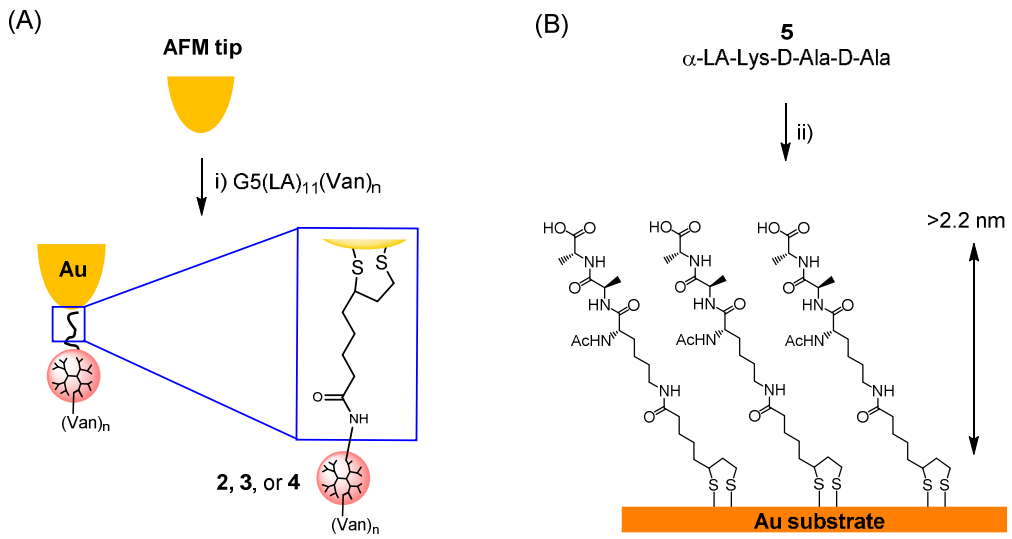

Reagents and conditions: (i) **2**–**4** G5(LA)$_{11}$(Van)$_n$ + 11-mercapto-1-undecanol (MUD), [G5 conjugate]:[MUD] = 1:20; (ii) EtOH, room temperature. LA = α-Lipoic amide

The force profiles between the dendrimer conjugate and the peptide surface **5** show an adhesion force curve, an extension followed by a rupture event, and curves with no binding events (Figure S6). Adequate washing of the peptide surface after overnight immobilization resulted in a significant decrease of the force curves showing an extension and a rupture event. We surmised that the latter events are likely due to unbound or loosely bound peptide molecules on the surface, which were removed by the gentle washing of the surface. Prior work has shown force profiles between a tethered vancomycin molecule on an AFM probe and a D-Ala-D-Ala surface to be primarily adhesions type forces.[58]

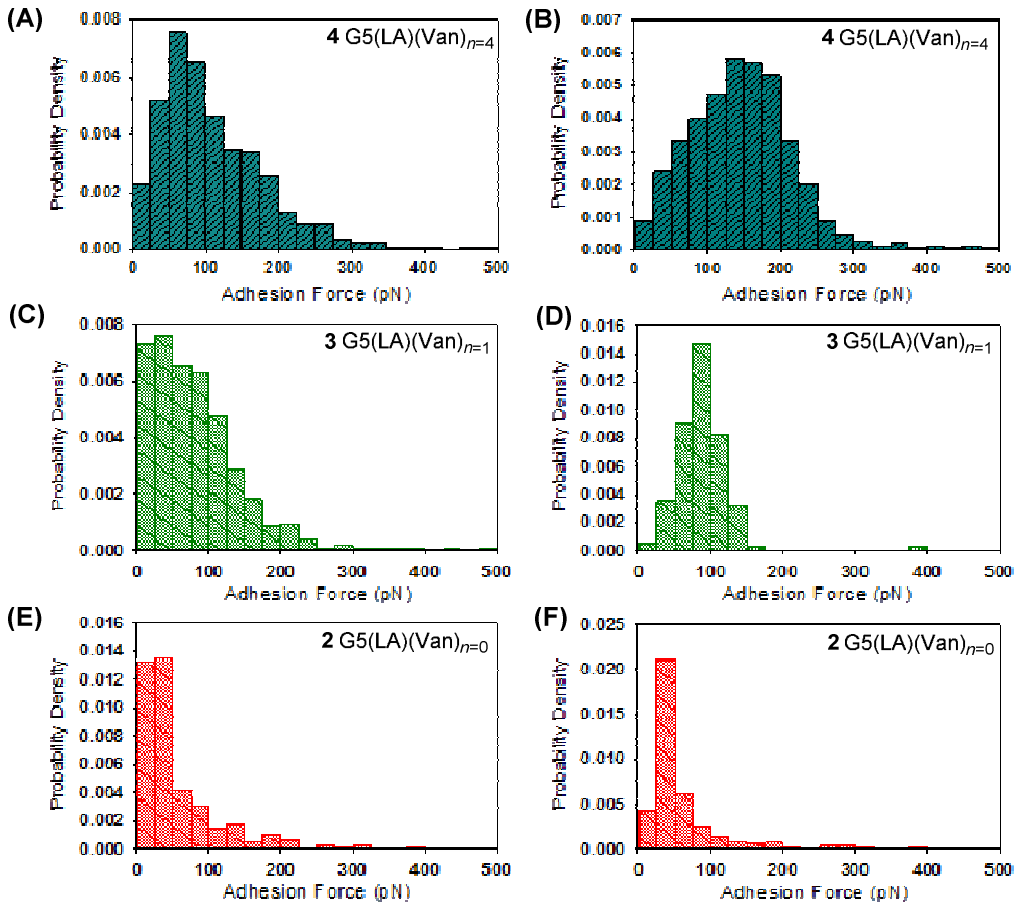

Figure 3. Adhesion force histograms obtained at a pulling velocity of 1030 nm/s (left panel) and 4880 nm/s (right panel) between **2**–**4** G5(LA)$_{11}$(Van)$_n$ (n = 0, 1, 4) and the α–LA-Lys-D-Ala-D-Ala peptide surface **5** in PBS buffer (pH 7.4).

The adhesion force distribution between **2**–**4** G5(LA)$_{11}$(Van)$_n$ (valency n = 0, 1, 4) and the peptide surface **5** is shown by the histograms in Figure 3 at pulling velocities of 1030 nm/s (left panel), and 4880 nm/s (right panel). The wider distributions observed for **4** (n = 4) are likely from multivalent cooperative binding of vancomycin due to the distribution of vancomycin molecules attached to an identical dendrimer (n = 1–9). The narrower distribution observed for **2** (n = 0) highlights the high density of non-specific interactions between the G5 dendrimer and the

peptide surface. While non-specific interactions were not observed in the SPR study, they were more prominent here due to the fact that the AFM force-pulling measurement is a stochastic binding event with a single dendrimer-surface interaction observed with each touch. At the higher pulling velocity, the mean adhesion force scales with **4** (n = 4) > **3** (n = 1) > **2** (n = 0). At the lower pulling velocity, **4** (n = 4) shows a higher density of adhesion forces between 100–300 pN compared to **3** (n = 1), with a higher average adhesion force for the former. The AFM force pulling data confirm that the binding avidity of **4** (n = 4) to the D-Ala-D-Ala surface is greater compared to **3** (n = 1).

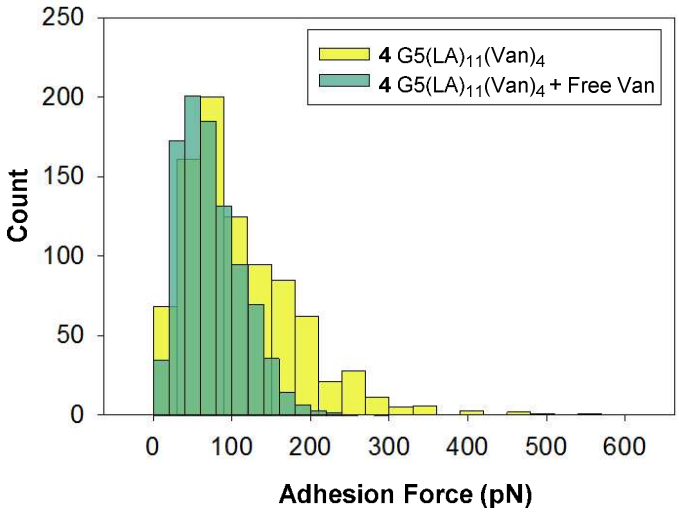

Figure 4. A control experiment showing the reduction in the frequency of adhesion force curves when the force-pulling measurements between **4** G5(LA)$_{11}$(Van)$_n$ (n = 4) and the D-Ala-D-Ala peptide surface were performed in the presence of free vancomycin (0.2 mg/mL). Pulling velocity = 1030 nm/s.

While the histogram data in Figure 3 show that the adhesion force distributions for **3**, **4** G5(LA)$_{11}$(Van)$_n$ (n = 1, 4) are different from those for **2** G5(LA)$_{11}$(Van)$_n$ (n = 0), a positive control was performed by introducing free vancomycin (0.2 mg/mL, 0.14 mM) to confirm the specificity of this interaction. The ~41% reduction in the adhesion events observed in the 100–

300 pN region between **4** (n = 4) and the D-Ala-D-Ala peptide surface in Figure 4 is attributed to the binding of free vancomycin to the peptide surface. Thus, the adhesion force distribution observed in the presence of free vancomycin is likely due to non-specific interactions. Moreover, the force profile is similar to the force distributions observed between **2** (n = 0) and the D-Ala-D-Ala peptide surface. This similarity is not surprising since **2** (n = 0) lacks any vancomycin molecules that could engage in specific interactions with the peptide surface. These non-specific interactions are also present in high density in the adhesion force distributions between **3**, **4** (n = 1, 4) and the D-Ala-D-Ala peptide surface. We attribute this to the interactions between the surface of the dendrimer conjugate (n = 1, 4) and the peptide surface.

Our previous work on dendrimer conjugated ligands and receptor systems have shown that the ligand-receptor binding force is dependent on the loading rate.[25] The adhesion force was measured at variable loading rates that ranged from 2500 to 50,000 pN/s. At each loading rate, force distribution plots were produced, and the adhesion force corresponding to the conjugate/D-Ala-D-Ala interaction was obtained by modeling the data with Gaussian functions as has been previously described.[25] Adhesion forces less than 100 pN were considered as primarily arising from non-specific interactions between the G5 dendrimer and the peptide surface, and they were not considered in the loading rate dependency study of **2**, **3**, **4** (n = 0, 1, 4).

The force spectrum of the dendrimer conjugate versus the D-Ala-D-Ala peptide surface is shown in Figure 5. The non-specific interactions between **2** (n = 0) and the peptide surface show very little dependency of the adhesion force with increasing loading rate. The adhesion force distribution for **2** (n = 0) shows a dominant low force peak and higher force peak (both <100 pN) (Figure S7). Both of these peaks arise from non-specific interactions and are not representative of the recognition interaction between vancomycin and the peptide surface. While the lower

forces (< 30 pN) are within the noise of the system, the forces measured between 30-100 pN are adhesion forces likely from electrostatic or van der Waals interactions, as previously observed between G5 dendrimer and receptor surfaces.[25]

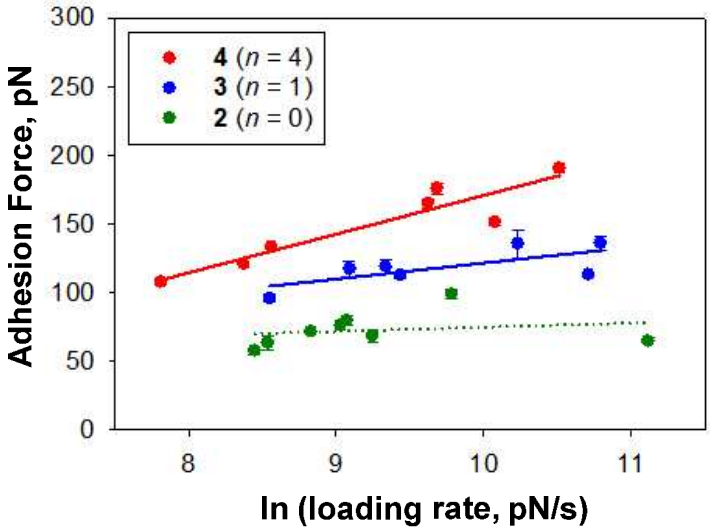

Figure 5. Dynamic force spectra of **2–4** G5(LA)$_{11}$(Van)$_n$ (n = 0, 1, 4) vs D-Ala-D-Ala peptide surface. The error presented is the standard error of the corresponding Gaussian peak fitted to the adhesion force and loading rate distributions. The dynamic force spectrum was modeled by the one-barrier Bell-Evans model (red and blue circles). A linear fit was added to the **2** (n = 0) data set to guide the eye.

The adhesion interactions between **3** (n = 1) and the D-Ala-D-Ala peptide surface in the force spectrum (Figure 5) show a loading rate dependency, with mean adhesion forces ranging from 96 pN to 136 pN. This corresponds well with a previous study that examined the adhesion force between a single vancomycin tethered to an AFM tip and a D-Ala-D-Ala peptide surface.[58] In that study, the mean adhesion force was estimated to be ~98 pN, while the mean adhesion force ranged from 98 to 125 pN for comparable loading rates as shown in Figure 5. Therefore, it is very likely that the results shown in Figure 5 for **3** (n = 1) are primarily from a single vancomycin molecule attached to the dendrimer interacting with the peptide surface. The force

spectrum data were fitted using the phenomenological Bell-Evans expression,[67, 68] $F^* = \left(\frac{k_\beta T}{\chi_\beta}\right)\ln\left(\frac{r k_{off}^{-1}\chi_\beta}{k_\beta T}\right)$, where F^* is the most probable adhesion force, $k_\beta T$ is the thermal energy, χ_β is the barrier width, k_{off} is the kinetic off-rate constant, and r is the force loading rate. The linear regime of a plot of F^* versus ln(r) is interpreted as a single activation energy barrier that can be characterized by the parameters χ_β and k_{off}. For **3** (n = 1) vs D-Ala-D-Ala peptide surface, the barrier width (χ_β) was found to be 0.35 ± 0.12 nm and the kinetic off-rate (k_{off}) was found to be 0.055 ± 0.018 s^{-1}. In comparison, previously reported data from single molecule force spectroscopy for the vancomycin vs D-Ala-D-Ala peptide surface found a barrier width of ~ 0.36 nm and a k_{off} value of ~0.002 s^{-1}.[58] The kinetic off-rate constant for **3** (n = 1) is a factor of 27 higher compared to the vancomycin tethered to an AFM tip. However, a comparison of the k_{off} value between the SPR measurements (Table 2) and the AFM measurements show good agreement, where its SPR k_{off} value is only a factor of 2 greater than the k_{off} value obtained from AFM for the **3** (n = 1) vs D-Ala-D-Ala peptide surface.

The mean adhesion force measured for **4** (n = 4) is clearly greater than the mean adhesion force measured for **3** (n = 1) at all loading rates (Figure 5). For the dendrimer conjugate **4,** at very low loading rates, it appears that the binding interaction may be facilitated by a single vancomycin molecule, while at higher loading rates the binding appears to be cooperative with at least 2 vancomycin molecules on the G5 dendrimer interacting with the peptide surface. Although we modeled **4** (n = 4) for its loading rate dependency data with the Bell-Evans model,[67, 68] the barrier width of 0.14 nm and a k_{off} value of ~1.8 s^{-1} is not a good representation of the kinetics due to different binding avidities present as a function of the loading rate. However, the higher adhesion forces measured for the **4** (n = 4)/peptide system do correspond

well with the measurements from SPR, where the binding avidity is orders of magnitude stronger compared to the **3** (n = 1)/peptide system. Despite the use of stochastically generated G5 dendrimers with mean vancomycin valency, we have demonstrated that adhesion forces scale according to **4** (n = 4) > **3** (n = 1) > **2** (n = 0), and the kinetic parameters obtained for the monovalent **3** (n = 1)/peptide system corresponds well with its SPR results.

CONCLUSIONS

Here, we designed vancomycin-conjugated dendrimers as a class of bacterial cell wall-specific nanoconjugates and investigated their biophysical characteristics of multivalent binding by SPR and AFM spectroscopy. First, the vancomycin-conjugated PAMAM dendrimer was co-modified with LA such that its disulfide terminus provided a mechanism for the conjugate attachment to the surface of a gold-coated AFM tip through thiol-Au chemisorption. Use of this design strategy enabled to study an identical conjugate for its avidity and adhesion force by both AFM and SPR methods.

Second, the present SPR analysis of **4** G5$(LA)_{11}(Van)_n$ (n = 4) is indicative of its very tight binding (K_D = 0.34 nM) to a model surface immobilized with D-Ala-D-Ala. It indicates an enhancement of binding avidity by three orders of magnitude over free vancomycin, which is in good agreement with the K_D value of 0.25 nM[19] by a representative multivalent conjugate G5$(Van)_{5.8}$ which is similarly designed but lacks the LA moiety in the peripheral surface.

Third, the AFM study enabled us to gauge the physical forces of multivalent binding for this class of conjugates. Results from **4** indicate that this multivalent conjugate adheres to a D-Ala-D-Ala surface with forces greater than a monovalent conjugate **3** G5$(LA)_{11}(Van)_n$ (n = 1). Blocking experiments using free vancomycin were used to demonstrate that adhesion forces of <100 pN

were largely due to non-specific interactions between the dendrimer conjugate and the peptide surface. A loading rate dependence study was performed to estimate the kinetic parameters for **2**–**4** G5(LA)$_{11}$(Van)$_n$/peptide system. While **3**, **4** (n = 1, 4) showed a loading rate dependency, **2** (n = 0) showed little to no loading rate dependency. Kinetic parameters measured for **3** (n = 1)/peptide interactions correspond well with its k_{off} value obtained from SPR measurements, as well as with a prior study between vancomycin and a D-Ala-D-Ala peptide surface.[58]

Finally, in addition to its significant implication in the quantitative analysis of multivalent interaction, this study suggests practical applicability of bacteria-targeted NPs. For example, the multivalent conjugate validated here can be used as the AFM probe for drawing the topographical maps[69, 70] of the bacterial surface based on the dendrimer-cell wall peptide interaction, and for the real-time imaging of the cell-wall biosynthesis and maturation in live cells. Future efforts will be focused on advancing our technical capability for such applications.

EXPERIMENTAL SECTION

Materials

All reagents and solvents were purchased from commercial suppliers and used as received. These include (±)-α-lipoic acid (≥98%), vancomycin hydrochloride (≥80% by HPLC), and N^{α}-Ac-Lys-D-Ala-D-Ala (≥95%), *N*-hydroxybenzotriazole (HOBt), *N*,*N*′-diisopropyl-*N*-ethylamine (DIPEA), *N*-(3-dimethylaminopropyl)-*N*′-ethylcarbodiimide hydrochloride (EDC), all from Sigma-Aldrich, and benzotriazol-1-yl-oxytripyrrolidinophosphonium hexafluorophosphate (PyBOP) from Bachem. Ethanol (absolute, 200 proof) was purchased from AAPER Alcohol and Chemical Company. Potassium dichromate ($K_2Cr_2O_7$), purchased from Baker Chemical Company, was used in the preparation of chromic acid solutions. Nanopure (NP) water (18.2 MΩ

cm^{-1} resistivity) was obtained from a Barnstead water purifier (Fischer Scientific). A fifth generation (G5) PAMAM dendrimer G5(NH_2)$_n$ (theoretical n = 128)[46] was purchased as a solution in methanol (17.5%) from Dendritech, Inc. Prior to derivatization, its trailing generations contained as impurities were removed by dialysis against deionized water in a membrane tubing (MWCO 10 kDa). The number (n) of primary amines per dendrimer was determined as 114 (experimental) by potentiometric titration as reported.[71]

Synthesis of 2–4 G5(LA)$_m$(Van)$_n$ Conjugates (Scheme 1)

Pre-activation of lipoic acid. To a mixture of (±)-α-lipoic acid (14 mg, 67.4 μmol) and HOBt (10 mg, 67.4 μmol) dissolved in anhydrous DMF (2 mL) was added DIPEA (23.5 μL, 135 μmol) and EDC (26 mg, 135 μmol). The final mixture was stirred at room temperature for 12 h, and it was used in the next step without further treatment.

Pre-activation of vancomycin. A solution of vancomycin hydrochloride (22.2 mg, 15 μmol) and HOBt (2.4 mg, 15.7 μmol) in DMSO (1.5 mL) was prepared and diluted with DMF (0.5 mL). To this solution was added DIPEA (5.5 μL, 31.4 μmol) and PyBOP (8.2 mg, 15.7 μmol). The reaction mixture was stirred for 30 min at room temperature, and it was used in the step for dendrimer conjugation.

1 G5(LA)$_m$. To a solution of G5(NH_2)$_{n\,=\,114}$ (120 mg, 4.5 μmol) dissolved in methanol (20 mL) was added the solution of pre-activated lipoic acid (LA) (67.4 μmol) prepared above. The mixture was stirred at room temperature for 2 h, and it was divided equally into three portions, each ~7.3 ml (equivalent to 40 mg dendrimer).

2–4 G5(LA)$_m$(Van)$_n$: To each solution of G5(LA)$_m$ (7.3 mL) was added a varying amount of the activated vancomycin solution prepared above: aliquot = 0 (none) for **2**; 0.4 mL for **3**; 1.6 mL for **4**. After stirring for 12 h, DIPEA (52.2 μL, 299 μmol) and glutaric anhydride (25.6 mg, 225 μmol) were added to each reaction mixture. Each reaction mixture was stirred at room temperature for additional 12 h, and the solution was concentrated *in vacuo*. The residue was dissolved in water (2 mL), loaded in a dialysis membrane tube with the molecular weight cut-off (MWCO) of 10,000 Da, and dialyzed exhaustively against water (2 × 1.0 L), PBS buffer, pH 7.4 (1 L) and water (2 × 1.0 L). The solution in the tube was collected and further purified by centrifugal filtration (MWCO 10,000 Da) using PBS buffer (3 × 2 mL) and then water (3 × 2 mL), each as an eluent. The solution in the top container of the tube was collected and freeze-dried to afford 47 mg (**2**), 55 mg (**3**), and 61 mg (**4**). Polymer purity ≥95% (**2**, **3**, **4**). UPLC: t_r = 7.1 min (**2**), 7.0 min (**3**), 7.0 min (**4**). GPC: t_r = 23.4 min (**2**), 23.0 min (**3**), 24.1 min (**4**). MALDI–ToF (*m/z*, gmol^{-1}): 36,600 (**2**), 36,900 (**3**), 41,600 (**4**). UV–vis (PBS, pH 7.4): λ_{max} = 282 nm for **3** or **4** (ε = 6,652 M^{-1}cm^{-1}). ^{1}H NMR (500 MHz) for **2** (D_2O)**:** δ 3.67 (s), 3.35 (br, s, strong), 3.34 (s, strong), 3.30 (s, strong), 3.24–3.16 (m, weak), 2.94 (br, s, strong), 2.88 (s, strong), 2.77 (br, s, strong), 2.61 (m, weak), 2.48 (br, s, strong), 2.41–2.38 (t, J_1 =5 Hz, weak), 2.24–2.21 (t, J_1 =5 Hz, strong), 2.18–2.15 (t, J_1 =5 Hz, strong), 1.87–1.86 (m, weak), 1.83–1.77 (m, strong), 1.59–1.58 (m, weak), 1.38 (m, weak), 1.20–1.17 (m, weak) ppm. **3** (D_2O): δ 3.67 (s), 3.49 (br, s), 3.34 (s, strong), 3.29 (s, strong), 3.14 (br, s), 2.92 (br, strong), 2.88 (s, strong), 2.72 (br, strong), 2.46 (br, s, strong), 2.24–2.21 (t, J_1 =5 Hz, strong), 2.18–2.15 (t, J_1 =5 Hz, strong), 2.03–1.96 (m, weak), 1.87–1.86 (m, weak), 1.83–1.79 (m, strong), 1.58 (br, s, weak), 1.38 (br, s, weak), 1.20–1.14 (m, weak) ppm. **4** (D_2O): δ 7.61 (br, weak), 7.38 (br, weak), 7.10 (br, weak), 6.51 (br, weak), 6.20 (br, weak), 5.66 (br, weak), 5.40 (br, weak), 3.73, (br, weak), 3.67 (s), 3.49

(br, s), 3.34 (s, strong), 3.29 (s, strong), 3.14 (br, s), 3.00 (s, weak), 2.90 (br, strong), 2.88 (s, strong), 2.71 (br, strong), 2.46 (br, s, strong), 2.22–2.21 (m, strong), 2.17–2.15 (m, strong), 2.02–1.96 (m, weak), 1.87–1.86 (m, weak), 1.81–1.78 (m, strong), 1.58 (br, s, weak), 1.37 (br, s, weak), 1.27–1.18 (m, weak), 0.89 (br, s, weak) ppm. Abbreviation: s = singlet, t = triplet, m = multiplet, br = broad

The valency (*m*) of the lipoic amide molecule attached to the conjugate G5(LA)$_m$(Van)$_n$ was determined on a mean basis by an NMR integration method in which the CH_2 signals of LA (δ 1.0–1.4 ppm) were compared to the reference CH_2 signals of glutarate at δ 1.7 and 2.0–2.2 ppm (108 CH_2 residues per dendrimer), yielding m = 11 (±1). The valency (*n*) of vancomycin molecules attached to each conjugate was determined on a mean basis by the analysis of UV–vis absorption at λ_{max} 282 nm (vancomycin): n = 1 (**3**); n = 4 (**4**).

Synthesis of 5 α-LA-Lys-D-Ala-D-Ala

Preparation of α-lipoic acid *p*-nitrophenyl (NP) ester: To a cold solution of α-lipoic acid (200 mg, 0.969 mmol) and *p*-nitrophenol (148 mg, 1.07 mmol) dissolved in dichloromethane (5 mL) in an ice bath was added dicyclohexylcarbodiimide (220 mg, 1.07 mmol). This mixture was stirred in the ice bath for 30 min and then at ambient temperature for 6 h. It was diluted by adding 10 mL of dichloromethane and white precipitates were removed by filtration. The filtered solution was washed with a cold sodium bicarbonate solution, dried with sodium sulfate, and concentrated *in vacuo*. The crude product was purified by silica column chromatography by eluting with a mixture of ethyl acetate and hexane (1:3). The product was obtained as pale yellow solid (87 mg, 27%). R_f (1:3 EtOAc/hexane) = 0.5. ^{1}H NMR (500 MHz, $CDCl_3$): δ 8.28–8.26 (d, J = 10 Hz, 2H, $C_6H_4NO_2$), 7.29–7.27 (d, J = 10 Hz, 2H, $C_6H_4NO_2$), 3.62–3.55 (m, 1H,

CH), 3.22–3.08 (m, 2H), 2.64–2.62 (t, J = 5 Hz, 2H), 2.50–2.46 (m, 2H), 1.94–1.86 (m, 2H), 1.84–1.72 (m, 2H), 1.69–1.52 (m, 2H) ppm.

To a solution of N^{α}-acetyl-lysine-D-alanine-D-alanine (5.0 mg, 15.1 μmol) dissolved in DMF (0.5 mL) was added triethylamine (42 μL, 30.3 μmol), and then the lipoic acid *p*-nitrophenol ester (5.9 mg, 18.2 μmol). The final mixture was stirred at room temperature for 24 h. It was concentrated *in vacuo*, and its residue was purified by silica column chromatography by eluting with a mixture of dichloromethane in methanol. The product was obtained as white solid (5.6 mg, 72%). R_f (50% CH_3OH/CH_2Cl_2) = 0.45. HRMS (ESI): $[M + H]^+$ calcd for $C_{22}H_{39}N_4O_6S_2$, 519.2306, found, 519.2305. ^{1}H NMR (500 MHz, CD_3OD): δ 4.40–4.36 (q, J = 5 Hz, 1H), 4.28 (m, 2H), 3.61–3.55 (m, 1H), 3.20–3.16 (m, 3H), 3.13–3.08 (m, 1H), 2.50–2.44 (m, 1H), 2.21–2.18 (t, J = 5 Hz, 2H), 2.00 (s, 3H), 1.93–1.86 (m, 1H, CH), 1.82–1.56 (m, 6H), 1.55–1.49 (m, 2H), 1.48–1.43 (m, 2H), 1.42–1.36 (m, 8H) ppm. ^{13}C NMR (100 MHz, CD_3OD): δ 175.99, 174.20, 57.56, 55.09, 50.31, 41.31, 40.03, 39.34, 36.92, 35.74, 32.44, 30.08, 29.89, 26.78, 24.23, 22.47, 18.33, 17.96 ppm.

Methods

Surface Plasmon Resonance (SPR) Spectroscopy. SPR experiments for vancomycin-conjugated PAMAM dendrimers were performed in a Biacore® X model (Pharmacia Biosensor, AB) using a CM5 sensor chip as reported.[19, 72] The flow cell 1 (FC_1) of the sensor chip was treated for the immobilization of a N^{α}-Ac-Lys-D-Ala-D-Ala peptide, while its flow cell 2 (FC_2) was treated without the peptide to be used as a reference cell. The peptide immobilization was performed following an amide coupling method using EDC/NHS (1:1 mixture of 0.4 M EDC

and 0.1 M NHS, each in water; 70 μL) in which the peptide was covalently attached at its *N*-terminus to the layer of carboxymethylated dextran on the surface.

For a typical SPR binding experiment, vancomycin or its conjugate was dissolved and serially diluted in HBS–EP buffer, and its aliquot of 50 μL was injected at a flow rate of 20 μL/min. The data were collected until the dissociation trace returned to a flat baseline or the end of each dissociation phase (t ≥600 s). The surface regeneration of the sensor chip was performed by treatment with 10 μL of 10 mM glycine–HCl, pH 2.5.

SPR data processing and analysis. The value of response unit (RU_1) recorded from FC_1 was subtracted with the value of the reference response unit (RU_2) from FC_2 to correct the contribution from a bulk effect and non-specific adhesion: ΔRU (corrected) = $RU_1 - RU_2$. Two rate constants—association (on) rate constant (k_{on}) and dissociation (off) rate constant (k_{off})—were extracted by fitting each corrected sensorgram to the Langmuir model and using a global curve fitting model.[54]

$$RU_t = RU_{eq} \times e^{-(k_{off} t)} \text{ (dissociation phase)}$$

$$RU_t = RU_{eq} \times (1 - e^{-[(k_{on} \times C + k_{off})(t - t_0)]}) \text{ (association phase)}$$

$k_{on} = (k_s - k_{off})/C$ (where C refers to the concentration of analyte)

A value for equilibrium dissociation constant K_D (= k_{off}/k_{on}) was calculated from each pair of its rate constants, and a mean value was calculated from multiple independent measurements (N ≥ 4).

Surface Preparation for AFM Force Pulling. α-LA-Lys-D-Ala-D-Ala **5** (MW 518.22 g/mol, 0.34 mg) was dissolved in 1 mL of ethanol, which was filtered (0.22 μm pore size) prior to use. The solution was aliquoted into 100 μL and 10 μL portions and frozen. Ultraflat template-stripped gold surfaces, prepared as described elsewhere,[25, 26] were incubated in THF for approximately 4 minutes. The mica layer was stripped, revealing an ultra-flat gold surface. The gold surface was washed three times with NP water and ethanol. The surface was then immediately placed in a 1 μM solution of **5** in ethanol and allowed to incubate overnight. Prior to AFM measurements, the peptide surface was rinsed three times with NP water, upon removal, and affixed to a stainless steel puck.

Tip Preparation for AFM Force Pulling. Standard silicon nitride OBL gold-coated cantilevers, (Bruker, Camarillo, CA, nominal length 60 μm) were cleaned with a hot solution of chromic acid (17 mg/mL, 3 minute incubation) and rinsed thoroughly with NP water. The AFM cantilever was incubated overnight in a 1-mL ethanol solution containing **2**–**4** G5$(LA)_{11}(Van)_n$ (n = 0, 1, 4) to 11-mercapto-1-undecanol (1:20). As a note, solutions of the conjugates **2** and **3** were prepared using ethanol; the conjugate **4** was dissolved in PBS buffer because of its poor solubility in ethanol. After incubation, the tip was rinsed thoroughly with NP water and placed in a fluid cell for force spectroscopy measurements.

Atomic Force Spectroscopy Instrumentation. Force spectroscopy measurements were performed with a PicoForce MultiMode 8 AFM (Bruker, Santa Barbara, CA) equipped with a 40 μm scanner (20 μm z direction). Spring constants of the tips were determined using the thermal fluctuation method. Spring constants ranged from 19.0 to 22.3 pN/nm.

Force Spectroscopy Measurements. Force spectroscopy experiments were performed at room temperature (23 °C) in a glass fluid cell in PBS. A ramp size of 250 nm, a trigger threshold of 100 pN, and a surface delay of 500 ms were used for all force pulling experiments. Tip velocity was varied from 407 nm/s to 4880 nm/s for the conjugate **3**. For conjugates **2** and **4**, forward tip velocity was kept constant at 1030 nm/s, and reverse tip velocity was varied from 201 nm/s to 4880 nm/s. Force measurements were taken at 25 locations within a 1 μm^2 area for each tip velocity. Fifty AFM force curves were captured at each location for a total of 1250 force curves for a given tip velocity. Blocking studies were carried out at a single tip velocity to examine the binding specificity between the dendrimer-conjugated vancomycin and the D-Ala-D-Ala surface; after a normal pulling experiment with the conjugate **4**, 0.2 mg/mL of free vancomycin was injected into the fluid cell and allowed to equilibrate for 30 minutes. Next, a force pulling experiment was conducted using a tip velocity of 1.03 μm/s.

Force Spectroscopy Analysis. Data analysis was performed with a Scanning Probe Image Processor (SPIP) software (version 6.6.2 Image Metrology A/S, Lyngby, Denmark). For both the loading rate dependence and the blocking study, force curves were filtered using the SPIP force curve analysis and batch processing modules. Baseline and hysteresis correction were performed on all force curves, and drag correction was only performed as required. A worm-like chain model was fitted to force curves displaying an adhesion or rupture event to determine the unbinding force and the apparent loading rate. The apparent loading rate was found through multiplication of the retraction pulling velocity and the slope of the force curve at the rupture point.

Distributions in the form of histograms for adhesion forces and apparent loading rates were generated for every tip velocity using SigmaPlot software (version 13.0 Systat Software, San Jose, CA). Gaussian curves were fitted to each loading rate distribution using PeakFit software (version 4.11 Systat Software, San Jose, CA); the peak value was recorded as the most probable loading rate for that unbinding event. The error of the most probable value was the standard deviation of the corresponding Gaussian peak at the 95% confidence interval.

Acknowledgements. This work was supported in part by the British Council and Department for Business Innovation & Skills through the Global Innovation Initiative (SKC). KS acknowledges the support of a Calvin Research Fellowship.

Supporting Information Available: Copies of spectra data are provided online. This material is available free of charge via the Internet at http://pubs.acs.org.

Author Contributions: The manuscript was written through contributions of all authors. All authors have given approval to the final version of the manuscript.

References

(1) Agasti, S. S.; Rana, S.; Park, M.-H.; Kim, C. K.; You, C.-C.; Rotello, V. M. Nanoparticles for detection and diagnosis. *Adv. Drug Delivery Rev.* **2010**, *62*, 316–328.

(2) Kamaly, N.; Xiao, Z.; Valencia, P. M.; Radovic-Moreno, A. F.; Farokhzad, O. C. Targeted polymeric therapeutic nanoparticles: design, development and clinical translation. *Chem. Soc. Rev.* **2012**, *41*, 2971–3010.

(3) Peer, D.; Karp, J. M.; Hong, S.; Farokhzad, O. C.; Margalit, R.; Langer, R. Nanocarriers as an emerging platform for cancer therapy. *Nat. Nanotechnol.* **2007**, *2*, 751–760.

(4) Majoros, I. J.; Williams, C. R.; Becker, A.; Baker Jr, J. R. Methotrexate Delivery *via* Folate Targeted Dendrimer-Based Nanotherapeutic Platform. *Wiley Interdiscip. Rev.: Nanomed. Nanobiotechnol.* **2009**, *1*, 502–510.

(5) Fasting, C.; Schalley, C. A.; Weber, M.; Seitz, O.; Hecht, S.; Koksch, B.; Dernedde, J.; Graf, C.; Knapp, E.-W.; Haag, R. Multivalency as a Chemical Organization and Action Principle. *Angew. Chem., Int. Ed.* **2012**, *51*, 10472–10498.

(6) Kiessling, L. L.; Gestwicki, J. E.; Strong, L. E. Synthetic Multivalent Ligands as Probes of Signal Transduction. *Angew. Chem., Int. Ed.* **2006**, *45*, 2348–2368.

(7) Mammen, M.; Choi, S. K.; Whitesides, G. M. Polyvalent Interactions in Biological Systems: Implications for Design and Use of Multivalent Ligands and Inhibitors. *Angew. Chem., Int. Ed.* **1998**, *37*, 2754–2794.

(8) Guo, Y.; Sakonsinsiri, C.; Nehlmeier, I.; Fascione, M. A.; Zhang, H.; Wang, W.; Pöhlmann, S.; Turnbull, W. B.; Zhou, D. Compact, Polyvalent Mannose Quantum Dots as Sensitive, Ratiometric FRET Probes for Multivalent Protein–Ligand Interactions. *Angew. Chem., Int. Ed.* **2016**, *55*, 4738–4742.

(9) Xu, L.; Josan, J. S.; Vagner, J.; Caplan, M. R.; Hruby, V. J.; Mash, E. A.; Lynch, R. M.; Morse, D. L.; Gillies, R. J. Heterobivalent ligands target cell-surface receptor combinations in vivo. *Proc. Natl. Acad. Sci. U. S. A.* **2012**, *109*, 21295–21300.

(10) Kane, R. S. Thermodynamics of Multivalent Interactions: Influence of the Linker. *Langmuir* **2010**, *26*, 8636–8640.

(11) Zhou, H.; Jiao, P.; Yang, L.; Li, X.; Yan, B. Enhancing Cell Recognition by Scrutinizing Cell Surfaces with a Nanoparticle Array. *J. Am. Chem. Soc.* **2011**, *133*, 680–682.

(12) Fu, F.; Wu, Y.; Zhu, J.; Wen, S.; Shen, M.; Shi, X. Multifunctional Lactobionic Acid-Modified Dendrimers for Targeted Drug Delivery to Liver Cancer Cells: Investigating the Role Played by PEG Spacer. *ACS Appl. Mater. Interfaces* **2014**, *6*, 16416–16425.

(13) Zheng, Y.; Fu, F.; Zhang, M.; Shen, M.; Zhu, M.; Shi, X. Multifunctional dendrimers modified with alpha-tocopheryl succinate for targeted cancer therapy. *MedChemComm* **2014**, *5*, 879–885.

(14) Zhu, J.; Xiong, Z.; Shen, M.; Shi, X. Encapsulation of doxorubicin within multifunctional gadolinium-loaded dendrimer nanocomplexes for targeted theranostics of cancer cells. *RSC Adv.* **2015**, *5*, 30286–30296.

(15) Hrkach, J.; Von Hoff, D.; Ali, M. M.; Andrianova, E.; Auer, J.; Campbell, T.; De Witt, D.; Figa, M.; Figueiredo, M.; Horhota, A.; Low, S.; McDonnell, K.; Peeke, E.; Retnarajan, B.; Sabnis, A.; Schnipper, E.; Song, J. J.; Song, Y. H.; Summa, J.; Tompsett, D.; Troiano, G.; Van Geen Hoven, T.; Wright, J.; LoRusso, P.; Kantoff, P. W.; Bander, N. H.; Sweeney, C.; Farokhzad, O. C.; Langer, R.; Zale, S. Preclinical Development and Clinical Translation of a PSMA-Targeted Docetaxel Nanoparticle with a Differentiated Pharmacological Profile. *Sci. Transl. Med.* **2012**, *4*, 128ra39.

(16) Zhu, J.; Fu, F.; Xiong, Z.; Shen, M.; Shi, X. Dendrimer-entrapped gold nanoparticles modified with RGD peptide and alpha-tocopheryl succinate enable targeted theranostics of cancer cells. *Colloids Surf., B* **2015**, *133*, 36–42.

(17) Zhu, J.; Zheng, L.; Wen, S.; Tang, Y.; Shen, M.; Zhang, G.; Shi, X. Targeted cancer theranostics using alpha-tocopheryl succinate-conjugated multifunctional dendrimer-entrapped gold nanoparticles. *Biomaterials* **2014**, *35*, 7635–7646.

(18) Sun, L.; Liu, D.; Wang, Z. Functional Gold Nanoparticle−Peptide Complexes as Cell-Targeting Agents. *Langmuir* **2008**, *24*, 10293–10297.

(19) Choi, S. K.; Myc, A.; Silpe, J. E.; Sumit, M.; Wong, P. T.; McCarthy, K.; Desai, A. M.; Thomas, T. P.; Kotlyar, A.; Banaszak Holl, M. M.; Orr, B. G.; Baker, J. R. Dendrimer-Based Multivalent Vancomycin Nanoplatform for Targeting the Drug-Resistant Bacterial Surface. *ACS Nano* **2013**, *7*, 214–228.

(20) Liao, Z.; Wang, H.; Lv, R.; Zhao, P.; Sun, X.; Wang, S.; Su, W.; Niu, R.; Chang, J. Polymeric Liposomes-Coated Superparamagnetic Iron Oxide Nanoparticles as Contrast Agent for Targeted Magnetic Resonance Imaging of Cancer Cells. *Langmuir* **2011**, *27*, 3100–3105.

(21) Wong, P. T.; Chen, D.; Tang, S.; Yanik, S.; Payne, M.; Mukherjee, J.; Coulter, A.; Tang, K.; Tao, K.; Sun, K.; Baker Jr, J. R.; Choi, S. K. Modular Integration of Upconversion Nanocrystal-Dendrimer Composites for Folate Receptor-Specific Near Infrared Imaging and Light Triggered Drug Release. *Small* **2015**, *11*, 6078–6090.

(22) Wang, L.; Liu, J.; Dai, Y.; Yang, Q.; Zhang, Y.; Yang, P.; Cheng, Z.; Lian, H.; Li, C.; Hou, Z.; Ma, P. a.; Lin, J. Efficient Gene Delivery and Multimodal Imaging by Lanthanide-Based Upconversion Nanoparticles. *Langmuir* **2014**, *30*, 13042–13051.

(23) Cao, P.; Tong, L.; Hou, Y.; Zhao, G.; Guerin, G.; Winnik, M. A.; Nitz, M. Improving Lanthanide Nanocrystal Colloidal Stability in Competitive Aqueous Buffer Solutions using Multivalent PEG-Phosphonate Ligands. *Langmuir* **2012**, *28*, 12861–12870.

(24) Girish, C. M.; Binulal, N. S.; Anitha, V. C.; Nair, S.; Mony, U.; Prasanth, R. Atomic force microscopic study of folate receptors in live cells with functionalized tips. *Appl. Phys. Lett.* **2009**, *95*, 223703.

(25) Leistra, A. N.; Han, J. H.; Tang, S.; Orr, B. G.; Banaszak Holl, M. M.; Choi, S. K.; Sinniah, K. Force Spectroscopy of Multivalent Binding of Riboflavin-Conjugated Dendrimers to Riboflavin Binding Protein. *J. Phys. Chem. B* **2015**, *119*, 5785–5792.

(26) Leroueil, P. R.; DiMaggio, S.; Leistra, A. N.; Blanchette, C. D.; Orme, C.; Sinniah, K.; Orr, B. G.; Banaszak Holl, M. M. Characterization of Folic Acid and Poly(amidoamine) Dendrimer Interactions with Folate Binding Protein: A Force-Pulling Study. *J. Phys. Chem. B* **2015**, *119*, 11506–11512.

(27) Beaussart, A.; El-Kirat-Chatel, S.; Sullan, R. M. A.; Alsteens, D.; Herman, P.; Derclaye, S.; Dufrêne, Y. F. Quantifying the forces guiding microbial cell adhesion using single-cell force spectroscopy. *Nat. Protoc.* **2014**, *9*, 1049–1055.

(28) Liang, M. N.; Smith, S. P.; Metallo, S. J.; Choi, I. S.; Prentiss, M.; Whitesides, G. M. Measuring the forces involved in polyvalent adhesion of uropathogenic Escherichia coli to mannose-presenting surfaces. *Proc. Natl. Acad. Sci. U. S. A.* **2000**, *97*, 13092–13096.

(29) Liu, J.; Weller, G. E. R.; Zern, B.; Ayyaswamy, P. S.; Eckmann, D. M.; Muzykantov, V. R.; Radhakrishnan, R. Computational model for nanocarrier binding to endothelium validated using in vivo, in vitro, and atomic force microscopy experiments. *Proc. Natl. Acad. Sci. U. S. A.* **2010**, *107*, 16530–16535.

(30) Lee, J.-J.; Jeong, K. J.; Hashimoto, M.; Kwon, A. H.; Rwei, A.; Shankarappa, S. A.; Tsui, J. H.; Kohane, D. S. Synthetic Ligand-Coated Magnetic Nanoparticles for Microfluidic Bacterial Separation from Blood. *Nano Lett.* **2014**, *14*, 1–5.

(31) Kell, A. J.; Stewart, G.; Ryan, S.; Peytavi, R.; Boissinot, M.; Huletsky, A.; Bergeron, M. G.; Simard, B. Vancomycin-Modified Nanoparticles for Efficient Targeting and Preconcentration of Gram-Positive and Gram-Negative Bacteria. *ACS Nano* **2008**, *2*, 1777–1788.

(32) Gu, H.; Ho, P.-L.; Tsang, K. W. T.; Wang, L.; Xu, B. Using Biofunctional Magnetic Nanoparticles to Capture Vancomycin-Resistant *Enterococci* and Other Gram-Positive Bacteria at Ultralow Concentration. *J. Am. Chem. Soc.* **2003**, *125*, 15702–15703.

(33) Leevy, W. M.; Gammon, S. T.; Johnson, J. R.; Lampkins, A. J.; Jiang, H.; Marquez, M.; Piwnica-Worms, D.; Suckow, M. A.; Smith, B. D. Noninvasive Optical Imaging of Staphylococcus aureus Bacterial Infection in Living Mice Using a Bis-Dipicolylamine-Zinc(II) Affinity Group Conjugated to a Near-Infrared Fluorophore. *Bioconjugate Chem.* **2008**, *19*, 686–692.

(34) Moison, E.; Xie, R.; Zhang, G.; Lebar, M. D.; Meredith, T. C.; Kahne, D. A Fluorescent Probe Distinguishes between Inhibition of Early and Late Steps of Lipopolysaccharide Biogenesis in Whole Cells. *ACS Chem. Biol.* **2017**, *12*, 928–932.

(35) Wong, P.; Tang, S.; Mukherjee, J.; Tang, K.; Gam, K.; Isham, D.; Murat, C.; Sun, R.; Baker, J. R.; Choi, S. K. Light-Controlled Active Release of Photocaged Ciprofloxacin for

Lipopolysaccharide-Targeted Drug Delivery using Dendrimer Conjugates. *Chem. Commun. (Cambridge, U. K.)* **2016**, *52*, 10357–10360.

(36) Sarker, P.; Shepherd, J.; Swindells, K.; Douglas, I.; MacNeil, S.; Swanson, L.; Rimmer, S. Highly Branched Polymers with Polymyxin End Groups Responsive to Pseudomonas aeruginosa. *Biomacromolecules* **2010**, *12*, 1–5.

(37) Han, M.-L.; Shen, H.-H.; Hansford, K. A.; Schneider, E. K.; Sivanesan, S.; Roberts, K. D.; Thompson, P. E.; Le Brun, A. P.; Zhu, Y.; Sani, M.-A.; Separovic, F.; Blaskovich, M. A. T.; Baker, M. A.; Moskowitz, S. M.; Cooper, M. A.; Li, J.; Velkov, T. Investigating the Interaction of Octapeptin A3 with Model Bacterial Membranes. *ACS Infect. Dis.* **2017**, *3*, 606–619.

(38) Metallo, S. J.; Kane, R. S.; Holmlin, R. E.; Whitesides, G. M. Using Bifunctional Polymers Presenting Vancomycin and Fluorescein Groups To Direct Anti-Fluorescein Antibodies to Self-Assembled Monolayers Presenting d-Alanine-d-Alanine Groups. *J. Am. Chem. Soc.* **2003**, *125*, 4534–4540.

(39) Sundram, U. N.; Griffin, J. H.; Nicas, T. I. Novel Vancomycin Dimers with Activity against Vancomycin-Resistant Enterococci. *J. Am. Chem. Soc.* **1996**, *118*, 13107–13108.

(40) Walsh, C. Molecular Mechanisms that Confer Antibacterial Drug Resistance. *Nature (London, U. K.)* **2000**, *406*, 775–781.

(41) Rao, J.; Yan, L.; Xu, B.; Whitesides, G. M. Using Surface Plasmon Resonance to Study the Binding of Vancomycin and Its Dimer to Self-Assembled Monolayers Presenting d-Ala-d-Ala. *J. Am. Chem. Soc.* **1999**, *121*, 2629–2630.

(42) Butler, M. S.; Hansford, K. A.; Blaskovich, M. A. T.; Halai, R.; Cooper, M. A. Glycopeptide antibiotics: Back to the future. *J. Antibiot.* **2014**, *67*, 631–644.

(43) Healy, V. L.; Lessard, I. A. D.; Roper, D. I.; Knox, J. R.; Walsh, C. T. Vancomycin resistance in enterococci: reprogramming of the d-Ala–d-Ala ligases in bacterial peptidoglycan biosynthesis. *Chem. Biol. (Oxford, U. K.)* **2000**, *7*, R109–R119.

(44) Gu, H.; Ho, P. L.; Tong, E.; Wang, L.; Xu, B. Presenting Vancomycin on Nanoparticles to Enhance Antimicrobial Activities. *Nano Lett.* **2003**, *3*, 1261–1263.

(45) Arimoto, H.; Nishimura, K.; Hayakawa, I.; Kinumi, T.; Uemura, D. Multi-valent polymer of vancomycin: enhanced antibacterial activity against VRE. *Chem. Commun. (Cambridge, U. K.)* **1999**, 1361–1362.

(46) Tomalia, D. A.; Naylor, A. M.; William A. Goddard, I. Starburst Dendrimers: Molecular-Level Control of Size, Shape, Surface Chemistry, Topology, and Flexibility from Atoms to Macroscopic Matter. *Angew. Chem., Int. Ed.* **1990**, *29*, 138–175.

(47) Patri, A. K.; Kukowska-Latallo, J. F.; Baker Jr, J. R. Targeted drug delivery with dendrimers: Comparison of the release kinetics of covalently conjugated drug and non-covalent drug inclusion complex. *Adv. Drug Delivery Rev.* **2005**, *57*, 2203–2214.

(48) Svenson, S.; Tomalia, D. A. Dendrimers in biomedical applications--reflections on the field. *Adv. Drug Delivery Rev.* **2005**, *57*, 2106–2129.

(49) Wang, Y.; Shen, W.; Shi, X.; Fu, F.; Fan, Y.; Shen, W.; Cao, Y.; Zhang, Q.; Qi, R. Alpha-Tocopheryl Succinate-Conjugated G5 PAMAM Dendrimer Enables Effective Inhibition of Ulcerative Colitis. *Adv. Healthcare Mater.* **2017**, *6*, 1700276.

(50) Kong, L.; Alves, C. S.; Hou, W.; Qiu, J.; Möhwald, H.; Tomás, H.; Shi, X. RGD Peptide-Modified Dendrimer-Entrapped Gold Nanoparticles Enable Highly Efficient and Specific Gene Delivery to Stem Cells. *ACS Appl. Mater. Interfaces* **2015**, *7*, 4833–4843.

(51) Wong, P. T.; Tang, S.; Cannon, J.; Chen, D.; Sun, R.; Lee, J.; Phan, J.; Tao, K.; Sun, K.; Chen, B.; Baker, J. R.; Choi, S. K. Photocontrolled Release of Doxorubicin Conjugated through a Thioacetal Photocage in Folate-Targeted Nanodelivery Systems. *Bioconjugate Chem.* **2017**, *28*, 3016–3028.

(52) Witte, A. B.; Leistra, A. N.; Wong, P. T.; Bharathi, S.; Refior, K.; Smith, P.; Kaso, O.; Sinniah, K.; Choi, S. K. Atomic Force Microscopy Probing of Receptor-Nanoparticle Interactions for Riboflavin Receptor Targeted Gold-Dendrimer Nanocomposites. *J. Phys. Chem. B* **2014**, *118*, 2872–2882.

(53) He, X.; Alves, C. S.; Oliveira, N.; Rodrigues, J.; Zhu, J.; Bányai, I.; Tomás, H.; Shi, X. RGD peptide-modified multifunctional dendrimer platform for drug encapsulation and targeted inhibition of cancer cells. *Colloids Surf., B* **2015**, *125*, 82–89.

(54) de Mol, N. J.; Fischer, M. J. E., Kinetic and Thermodynamic Analysis of Ligand-Receptor Interactions: SPR Applications in Drug Development. In *Handbook of Surface Plasmon Resonance*, The Royal Society of Chemistry: Cambridge, U.K., 2008; Vol. 5, pp 123–172.

(55) Bizzarri, A. R.; Cannistraro, S. Atomic Force Spectroscopy in Biological Complex Formation: Strategies and Perspectives. *J. Phys. Chem. B* **2009**, *113*, 16449–16464.

(56) Lynch, S.; Baker, H.; Byker, S. G.; Zhou, D.; Sinniah, K. Single Molecule Force Spectroscopy on G-Quadruplex DNA. *Chem. - Eur. J.* **2009**, *15*, 8113–8116.

(57) Schotanus, M. P.; Aumann, K. S.; Sinniah, K. Using Force Spectroscopy To Investigate the Binding of Complementary DNA in the Presence of Intercalating Agents. *Langmuir* **2002**, *18*, 5333–5336.

(58) Gilbert, Y.; Deghorain, M.; Wang, L.; Xu, B.; Pollheimer, P. D.; Gruber, H. J.; Errington, J.; Hallet, B.; Haulot, X.; Verbelen, C.; Hols, P.; Dufrêne, Y. F. Single-Molecule Force Spectroscopy and Imaging of the Vancomycin/d-Ala-d-Ala Interaction. *Nano Lett.* **2007**, *7*, 796–801.

(59) Choi, S. K.; Thomas, T. P.; Leroueil, P. R.; Kotlyar, A.; Van Der Spek, A. F. L.; Baker, J. R. Specific and Cooperative Interactions between Oximes and PAMAM Dendrimers as Demonstrated by ^{1}H NMR Study. *J. Phys. Chem. B* **2012**, *116*, 10387–10397.

(60) Witte, A. B.; Timmer, C. M.; Gam, J. J.; Choi, S. K.; Banaszak Holl, M. M.; Orr, B. G.; Baker, J. R.; Sinniah, K. Biophysical Characterization of a Riboflavin-conjugated Dendrimer Platform for Targeted Drug Delivery. *Biomacromolecules* **2012**, *13*, 507–516.

(61) Mullen, D. G.; Banaszak Holl, M. M. Heterogeneous Ligand–Nanoparticle Distributions: A Major Obstacle to Scientific Understanding and Commercial Translation. *Acc. Chem. Res.* **2011**, *44*, 1135–1145.

(62) Silpe, J. E.; Sumit, M.; Thomas, T. P.; Huang, B.; Kotlyar, A.; van Dongen, M. A.; Banaszak Holl, M. M.; Orr, B. G.; Choi, S. K. Avidity Modulation of Folate-Targeted Multivalent Dendrimers for Evaluating Biophysical Models of Cancer Targeting Nanoparticles. *ACS Chem. Biol.* **2013**, *8*, 2063–2071.

(63) Tan, Y. H.; Schallom, J. R.; Ganesh, N. V.; Fujikawa, K.; Demchenko, A. V.; Stine, K. J. Characterization of protein immobilization on nanoporous gold using atomic force microscopy and scanning electron microscopy. *Nanoscale* **2011**, *3*, 3395–3407.

(64) Chen, G.; Ning, X.; Park, B.; Boons, G.-J.; Xu, B. Simple, Clickable Protocol for Atomic Force Microscopy Tip Modification and Its Application for Trace Ricin Detection by Recognition Imaging. *Langmuir* **2009**, *25*, 2860–2864.

(65) Akrami, M.; Balalaie, S.; Hosseinkhani, S.; Alipour, M.; Salehi, F.; Bahador, A.; Haririan, I. Tuning the anticancer activity of a novel pro-apoptotic peptide using gold nanoparticle platforms. *Sci. Rep.* **2016**, *6*, 31030.

(66) Xue, Y.; Li, X.; Li, H.; Zhang, W. Quantifying thiol–gold interactions towards the efficient strength control. *Nat. Commun.* **2014**, *5*, 4348.

(67) Bell, G. I. Models for the specific adhesion of cells to cells. *Science* **1978**, *200*, 618–627.

(68) Evans, E. Energy landscapes of biomolecular adhesion and receptor anchoring at interfaces explored with dynamic force spectroscopy. *Faraday Discuss.* **1998**, 1–16.

(69) Alsteens, D.; Trabelsi, H.; Soumillion, P.; Dufrêne, Y. F. Multiparametric atomic force microscopy imaging of single bacteriophages extruding from living bacteria. *Nat. Commun.* **2013**, *4*, 2926.

(70) Plomp, M.; Malkin, A. J. Mapping of Proteomic Composition on the Surfaces of Bacillus Spores by Atomic Force Microscopy-Based Immunolabeling. *Langmuir* **2008**, *25*, 403–409.

(71) Majoros, I. J.; Thomas, T. P.; Mehta, C. B.; Baker Jr, J. R. Poly(amidoamine) Dendrimer-Based Multifunctional Engineered Nanodevice for Cancer Therapy. *J. Med. Chem.* **2005**, *48*, 5892–5899.

(72) Wong, P. T.; Tang, S.; Tang, K.; Coulter, A.; Mukherjee, J.; Gam, K.; Baker, J. R.; Choi, S. K. A lipopolysaccharide binding heteromultivalent dendrimer nanoplatform for Gram negative cell targeting. *J. Mater. Chem. B* **2015**, *3*, 1149–1156.

TOC graphic